Dendritic Voltage and Calcium-Gated Channels Amplify the Variability of Postsynaptic Responses in a Purkinje Cell Model

ERIK DE SCHUTTER
Born-Bunge Foundation, University of Antwerp-UIA, B2610 Antwerp, Belgium

De Schutter, Erik. Dendritic voltage and calcium-gated channels amplify the variability of postsynaptic responses in a Purkinje cell model. *J. Neurophysiol.* 80: 504–519, 1998. The dendrites of most neurons express several types of voltage and Ca^{2+}-gated channels. These ionic channels can be activated by subthreshold synaptic input, but the functional role of such activations in vivo is unclear. The interaction between dendritic channels and synaptic background input as it occurs in vivo was studied in a realistic computer model of a cerebellar Purkinje cell. It previously was shown using this model that dendritic Ca^{2+} channels amplify the somatic response to synchronous excitatory inputs. In this study, it is shown that dendritic ion channels also increased the somatic membrane potential fluctuations generated by the background input. This amplification caused a highly variable somatic excitatory postsynaptic potential (EPSP) in response to a synchronous excitatory input. The variability scaled with the size of the response in the model with excitable dendrite, resulting in an almost constant coefficient of variation, whereas in a passive model the membrane potential fluctuations simply added onto the EPSP. Although the EPSP amplitude in the active dendrite model was quite variable for different patterns of background input, it was insensitive to changes in the timing of the synchronous input by a few milliseconds. This effect was explained by slow changes in dendritic excitability. This excitability was determined by how the background input affected the dendritic membrane potentials in the preceding 10–20 ms, causing changes in activation of voltage and Ca^{2+}-gated channels. The most important model variables determining the excitability at the time of a synchronous input were the Ca^{2+}-activation of K^+ channels and the inhibitory synaptic conductance, although many other model variables could be influential for particular background patterns. Experimental evidence for the amplification of postsynaptic variability by active dendrites is discussed. The amplification of the variability of EPSPs has important functional consequences in general and for cerebellar Purkinje cells specifically. Subthreshold, background input has a much larger effect on the responses to coherent input of neurons with active dendrites compared with passive dendrites because it can change the effective threshold for firing. This gives neurons with dendritic calcium channels an increased information processing capacity and provides the Purkinje cell with a gating function.

INTRODUCTION

Single neuron physiology and the functional properties of voltage-gated channels usually are studied in the slice preparation. It is not always clear, however, how such studies apply to the in vivo situation, where neurons may very well behave differently due to the presence of continuous background synaptic input (for Purkinje cells, see Fig. 1 of Jaeger and Bower 1994; for other neurons, see Destexhe et al. 1996; Paré and Lebel 1997). Theoretical studies have shown that background input changes the passive cable properties of dendrites, thus affecting synaptic integration (Bernander et al. 1991; Holmes and Woody 1989; Rapp et al. 1992). It also has been suggested that synaptic integration by a passive dendrite cannot explain the irregular firing observed in neurons in vivo (Softky and Koch 1993). Recently, it has become clear that most dendrites are not passive. Instead, dendritic Ca^{2+} channels have been demonstrated in many neurons, including cerebellar Purkinje cells (Llinás and Sugimori 1980a) and neocortical (Amitai et al. 1993) and hippocampal (Regehr and Tank 1992) pyramidal neurons. Several groups have used the slice preparation to show that subthreshold excitatory inputs can activate dendritic Ca^{2+} channels (Denk et al. 1995; Eilers et al. 1995; Magee and Johnston 1995; Markram and Sakmann 1994; Regehr and Tank 1992). A combined experimental and modeling study demonstrated that background synaptic input can modify the bursting discharges caused by dendritic Ca^{2+} channels in thalamic reticular neurons (Destexhe et al. 1996).

Despite all these experimental studies, the role of dendritic channels in synaptic integration remains unclear. Therefore a modeling approach was used to study the interaction of dendritic voltage- and Ca^{2+}-gated channels with background input in Purkinje cells. The realistic Purkinje cell model with active dendritic properties (De Schutter and Bower 1994a,b) is based on all available experimental data and is not specifically tuned to simulate the responses to synaptic inputs. Because it is actually quite successful in reproducing such responses, the model can be considered to have predictive power (De Schutter and Bower 1994b). For example, in the model focal parallel fiber activation leads to localized voltage-gated Ca^{2+} inflow in the spiny dendrite (De Schutter and Bower 1993, 1994c). This model prediction was confirmed experimentally by others who used confocal imaging (Eilers et al. 1995) or dual photon microscopy (Denk et al. 1995) to demonstrate Ca^{2+} inflow in the spiny dendrite caused by parallel fiber activation. The same model also showed that background inhibition is essential to obtain the normal irregular in vivo firing pattern of Purkinje cells (De Schutter and Bower 1994b) and that, in fact, on average the inhibitory synaptic current in the Purkinje cell dendrite exceeds the total excitatory parallel fiber synaptic current (Jaeger et al. 1997). These predictions were confirmed by blocking inhibition in vivo, which changes the Purkinje cell firing pattern to the typical regular in vitro one (Jaeger and Bower 1994) and by the use of a dynamic clamp in vitro (Jaeger and Bower 1996). Recently others also showed the importance of inhibition for the irregular spiking of Purkinje cells (Häusser and Clark 1997).

The present study extends these prior findings by an inves-

tigation of how the active dendrite integrates a coherent excitatory stimulus when it is combined with background synaptic excitation and inhibition. Preliminary reports of these results have been presented in abstract form (De Schutter 1995b; De Schutter and Bower 1992).

MODEL AND METHODS

Purkinje cell model

The compartmental Purkinje cell model has been described in detail elsewhere (De Schutter and Bower 1994a,b). The model is based on a reconstructed Purkinje cell (Rapp et al. 1994), discretized into 1,600 compartments. Two versions of this model are used: a completely passive one and one with an active dendrite but passive soma (see also De Schutter and Bower 1994c). The active dendrite compartments contained two types of Ca^{2+} channels, a P type (CaP) (Llinás et al. 1989) and a T type (CaT) (Kaneda et al. 1990); two types of Ca^{2+}-activated K^+ channels, a BK type (KCa) (Latorre et al. 1989) and a K2 type (K2) (Gruol et al. 1991); and a persistent K^+ channel. The proximal part of the dendrite contained in addition low densities of voltage-gated K^+ channels, i.e., the delayed rectifier Kdr (Gähwiler and Llano 1989; Gruol et al. 1991) and the A current (KA) (Gruol et al. 1991; Hounsgaard and Midtgaard 1988).

A passive soma was used, i.e., the simple spike generating Na^+ (Stuart and Häusser 1994) and K^+ channels were absent from the model. This allowed measurement of excitatory postsynaptic potentials (EPSPs) in the soma instead of trains of action potentials, which simplifies the statistical analysis of responses to synaptic input (De Schutter and Bower 1994c).

All simulations used the GENESIS software (Bower and Beeman 1995). GENESIS 2.1 simulation scripts can be downloaded from http://bbf-www.uia.ac.be/CEREBELLUM (SYNCHROPASS9.g script).

Synaptic input

Because of computational constraints, only a fraction of the parallel fiber inputs are represented in the model (De Schutter and Bower 1994b). The 1,474 background parallel fiber inputs (onto the same number of passive spines) corresponded to ~1% of the total granule cell input onto a rat Purkinje cell (Harvey and Napper 1991). A standard approximation that may compensate for the reduced number of excitatory inputs modeled is to increase the firing rate of these synapses (Rapp et al. 1992). It was shown previously that such an approximation is valid for the interspike interval distributions in the Purkinje cell model (De Schutter and Bower 1994b) and that the necessary increase in rate scales linearly with the inverse of the fraction of inputs simulated. The number of inhibitory inputs onto the dendrite was 1,695 (De Schutter and Bower 1994b), which probably is close to the real number of inputs (Jaeger et al. 1997; Sultan et al. 1995).

The model simulated the ''in vivo'' state of the neuron described in De Schutter and Bower (1994b). This state was evoked by background input consisting of random asynchronous excitatory (Poisson distribution, mean frequency 28 Hz) and inhibitory input (1 Hz). Such input caused the full model to fire simple spikes at a realistic rate of ~65 Hz. Note that the asynchronous input frequencies are arbitrary values, which need to be scaled for the number of inputs represented (see preceding text and De Schutter and Bower 1994b). The real activation rates of these inputs in vivo are not known. EPSPs were evoked by synchronously activating 200 excitatory synapses distributed equally over the dendrite after 400 ms of simulation (always denoted as *time 0* in the figures).

Data analysis

Responses to synchronous input were measured as the amplitude of the EPSP in the passive soma, i.e., the difference between somatic peak membrane potential and baseline membrane potential at the time of synaptic activation. Other commonly used measures, like the EPSP integral and half-width, showed similar variability as the EPSP amplitude. A dendritic spike was defined as a transient change of the somatic membrane potential that crossed −20 mV.

Autocorrelations

Part of the analysis in this report was based on the use of two different autocorrelations over time (Fig. 7*B*). The autocorrelation over time of the baseline membrane potential was computed by selecting consecutive reference points in the somatic membrane potential computed during a particular simulation run and correlating them to data points generated later by the same simulation. This was repeated over 400 different simulations, resulting in n = 300,000 for each point in Fig. 7*B*. Data for the autocorrelation over time of the peak EPSP potential were generated by first simulating a reference EPSP and then repeating the simulation with identical background input while activating the synchronous input at later times (Fig. 7*A*). The reference peak EPSP potential was then autocorrelated with the peak potentials of the later triggered EPSP (n = 400).

Suprathreshold EPSPs

In the discussion, I present a simple analysis of how postsynaptic variability determines the likelihood of an EPSP being suprathreshold, which is expressed as the fraction of suprathreshold EPSPs (Fig. 10). To emphasize the dendritic contribution to differences between active and passive dendrite models, a similar effective voltage threshold for the peak amplitude of the EPSP was used for both models (3.5 mV above the mean somatic baseline potential). Using a realistic voltage threshold for the passive model (taking into account the low baseline membrane potential: 13 mV) resulted in a shift of the response curve to the right (800 inputs required for a suprathreshold response) without changing the slope of the curve. The use of a voltage threshold for the peak amplitude of the EPSP underestimated the number of spikes that the full spiking model would generate (Koch et al. 1995) but required fewer simulations. Simulations with 250 different background input patterns were repeated for each number of synchronous inputs (range 0–320). The synchronous input was applied after 400 ms of simulation (denoted as *time 0*) or at 405 and 430 ms for a subset of 10 simulations. Identical background input patterns were used for each input size in both the passive and the active dendrite models.

RESULTS

This report studies the interaction between dendritic voltage and Ca^{2+}-gated channels and the continuous background synaptic input that neurons are assumed to receive in vivo, and how this interaction affects the integration of suprathreshold synaptic inputs. In a model as complex as the Purkinje cell model (De Schutter 1994), it is not easy to separate the effects of the synaptic input from those of the dendritic voltage-gated channels (Jaeger et al. 1997; see also later sections of this report). Therefore most of this study systematically compares the somatic responses of a purely passive Purkinje cell model to those of a model with an active dendrite. This strategy makes it possible to study the interactions between voltage-gated channels and background input without separating their respective effects and allows

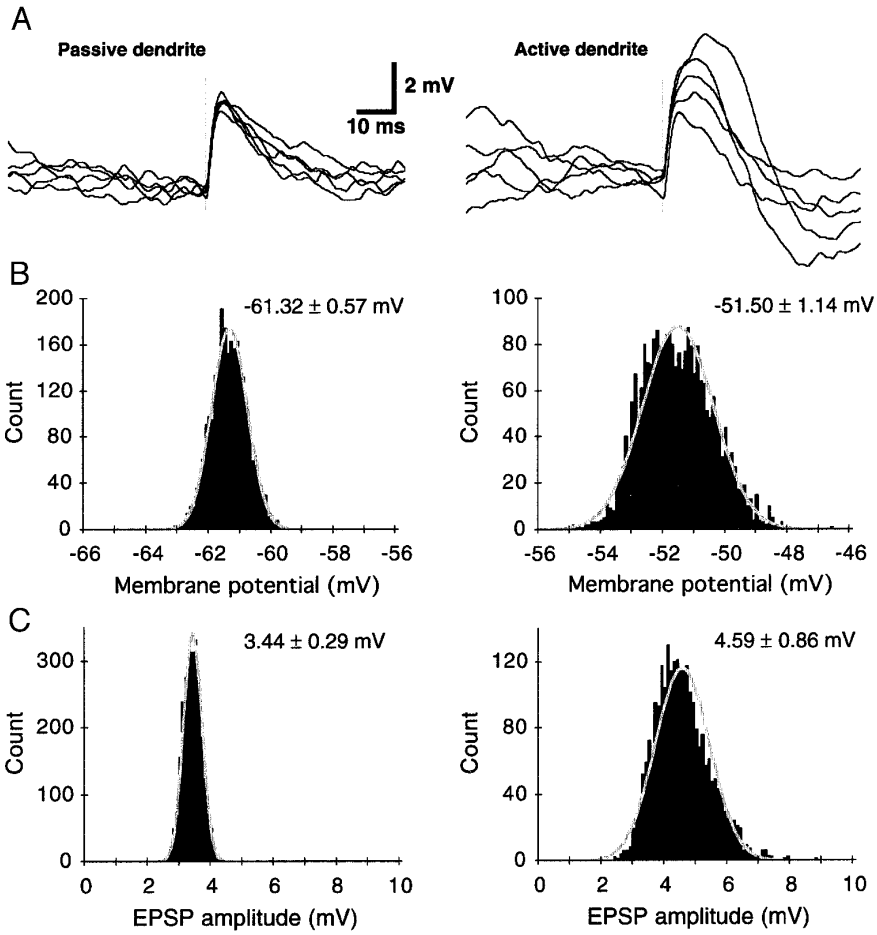

FIG. 1. Somatic membrane potential fluctuations and variability of the somatic excitatory postsynaptic potential (EPSP) in a passive membrane model (*left*) compared with an active dendrite model (*right*). *A*: examples of EPSPs recorded in the soma. Traces shown were selected to have similar membrane potentials at the time of the synchronous input. Note the large variability in amplitude and shape of EPSPs in the active dendrite model. *B*: distributions of somatic membrane potentials just before synchronous input (baseline membrane potential). Bars represent measured values; the mean ± SD is shown (n = 2,500). White curves show normal distribution with corresponding mean and SD. *C*: distributions of peak EPSP amplitudes, graphs as in *B*.

general statements about the properties of active dendrites to be made. In all simulations, both versions of the model received identical background and synchronous synaptic input so that any difference in the somatic response was entirely due to the presence of dendritic voltage- and Ca^{2+}-gated channels in the active dendrite model. Moreover, the study was restricted to the differences in somatic membrane potential fluctuations and in somatic EPSPs caused by synchronous excitatory inputs evenly distributed over the dendritic tree. Background input was simulated as randomly activated subthreshold excitatory and inhibitory inputs (De Schutter and Bower 1994b), also evenly distributed over the dendritic tree.

An example of typical responses is shown in Fig. 1*A*. The traces shown were selected to have approximately the same membrane potential at the time of the synchronous synaptic input so as to facilitate comparison of the EPSPs. Many differences between the active and passive dendrite models are apparent; I will first analyze the membrane potential fluctuations caused by the background input and then the somatic EPSP.

Difference between membrane potential in active and passive dendrites

The somatic membrane potential was always more depolarized in the active dendrite model than in the passive model: mean −51.50 mV compared with −61.32 mV (n = 2,500; Fig. 1*B*). This reflected the activation of a dendritic plateau potential (Llinás and Sugimori 1980a) by the background input in the active dendrite model (De Schutter and Bower 1994b). We have demonstrated previously in this model that, under the conditions simulated here, the tonically activated dendritic voltage-gated currents exceed the currents caused by the background synaptic input (Jaeger et al. 1997).

More surprising were the much larger membrane potential fluctuations in the active dendrite model compared with the passive one, as can be seen in Fig. 1*A*. This was confirmed by the much larger standard deviation (SD) of the membrane potential: 1.14 mV compared with 0.57 mV (Fig. 1*B*), a statistically significant difference ($P < 0.001$, 2-sided F test). Moreover, membrane potentials in the passive model were normally distributed ($P > 0.5$, χ^2), while they were not in the active model ($P < 0.001$). These fluctuations were (indirectly) caused by the Poisson background input as it was the only source of randomness in the model. In the passive dendrite model, the membrane potential fluctuations were the summation of many subthreshold synaptic potentials as demonstrated by their normal distribution. In the active model, however, the fluctuations cannot be explained by simple synaptic summation as they were not normally distributed. Moreover, one would expect synaptic potentials to be smaller in the active model because of the decreased input impedance due to the activation of voltage-gated channels (Bernander et al. 1991; Jack et al. 1975; Rapp et al.

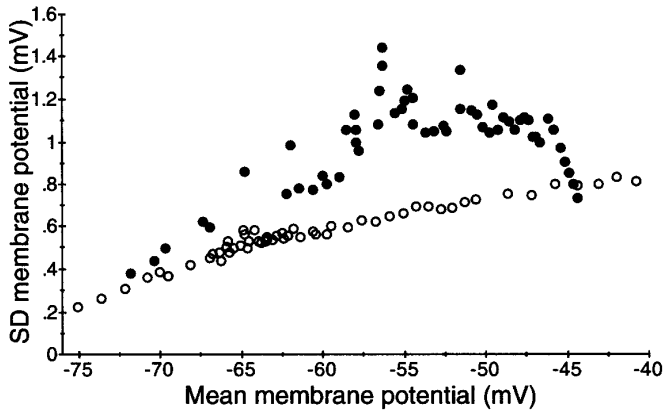

FIG. 2. Relation of somatic membrane potential fluctuations, measured as the SD, to the mean somatic membrane potential (n = 80,000) for passive dendrite (○) and active dendrite models (●). Different membrane potentials were obtained by changing the excitatory (range 6–90 Hz) and inhibitory (range 0.5–2.0 Hz) background input frequencies.

1992). Therefore, the larger membrane potential fluctuations in the active model were clearly caused by the (in)activation of dendritic voltage and Ca^{2+}-gated channels due to their interaction with the background input. In other words, the active dendrite amplified the variability of the membrane potential compared with a passive dendrite.

Voltage dependency of the amplification of variability

If the increased variability of the membrane potential is due to the activation of dendritic voltage-gated channels, it should be voltage dependent. Figure 2 compares the SD of the membrane potential of the active model versus that of the passive model for different mean somatic membrane potentials. Whenever the mean somatic membrane potential was between −65 and −46 mV, the variability of the membrane potential was much larger in the active dendrite model than in the passive one. This voltage range encompasses the activation threshold of the P-type dendritic Ca^{2+} channels present in the model (Regan 1991; Usowicz et al. 1992). But while the variability was voltage dependent, it was relatively constant within this voltage range. This was evident from the low correlation of the SD with somatic voltage in the active model (r = 0.43 in the range of −65 to −46 mV). Conversely, in the passive dendrite model these values were highly correlated (r = 0.96), which reflected the effect of the change in driving potential of (mainly the inhibitory) background input on the membrane potential fluctuations (e.g., Fig. 4*A*).

Figure 2 also demonstrates that the differences between active and passive model responses were robust over a wide range of physiologically relevant membrane potentials.

Variability of the somatic EPSPs

Next the suprathreshold response caused by the synchronous activation of 200 excitatory inputs was examined. It was shown previously that dendritic P-type Ca^{2+} channels amplify the somatic response of the model to such synchronous inputs (De Schutter and Bower 1994c). Here these results were confirmed: the mean amplitude of the EPSP was 4.59 mV in the active dendrite model compared with 3.44 mV in the passive one (Fig. 1*C*). But although the De Schutter and Bower study (1994c) considered only the averaged somatic EPSPs, it is clear from Fig. 1*A* that individual traces were quite noisy and variable in shape and amplitude. The variability was in both models completely and reproducibly determined by the background input patterns. A closer examination of Fig. 1*A* also shows that the EPSPs in the active dendrite model were much more variable in shape and amplitude than those in the passive model. For example, the EPSP peak membrane potential was −46.93 ± 1.36 mV in the active dendrite model and −57.88 ± 0.56 mV in the passive one ($P < 0.001$ for SD values, 2-sided F test). Moreover, the variability of the EPSP peak potential (SD 1.36 mV) was larger than that of the baseline for the active model (SD 1.14 mV, $P < 0.001$), whereas there was no significant difference for the passive model ($P > 0.2$). This means that the active dendrite model displayed a larger variability of the somatic response to synchronous input than the variability of the baseline membrane potential. In other words, the active dendrite amplified not only the size of the response but also its variability, whereas the passive dendrite amplified neither. The underlying mechanisms are explored later, but the difference in shapes of the EPSPs, in particular of the undershoot after the EPSP, already suggest that differential activation of Ca^{2+}-activated K^+ channels played an important role.

The difference in variability between active and passive dendrite models of the amplitude of the EPSP, as measured by its SD (0.86 vs. 0.29 mV, Fig. 1*C*), was also significant ($P < 0.001$, 2-sided F test) but smaller than the 0.80 mV difference found for the peak EPSP potential. This can be explained by the fact that the EPSP amplitude was measured as the difference between baseline and peak membrane potentials, values that were correlated positively, thus reducing the variability of their difference.

The active amplification of the variability of responses to synchronous synaptic input is the major finding of this study. It also can be described as a changing excitability of the active dendrite: the same synchronous input will sometimes be amplified much more than at other times. In the following sections, the robustness of these findings will be confirmed, their dependence on model parameters will be studied, and the causal factors in the model will be explored.

Size of the synchronous input

A first parameter that was studied is the number of synchronous inputs activated (Fig. 3). In both models, the response amplitude increased linearly over the range of activated inputs studied, which represented <1% of the parallel fibers contacting a Purkinje cell (Harvey and Napper 1991). In the passive dendrite, the SD of the response was constant ($P > 0.5$, 2-sided F test), i.e., independent of the size of the input and confirming the absence of any amplification. Therefore the interaction between background and synchronous inputs in the passive model can be described as additive or, in other words, as a coincidence effect. In the active dendrite model, however, the amplification mechanism increased both the mean response and its variability when ≥100 excitatory inputs were activated. The SD of responses

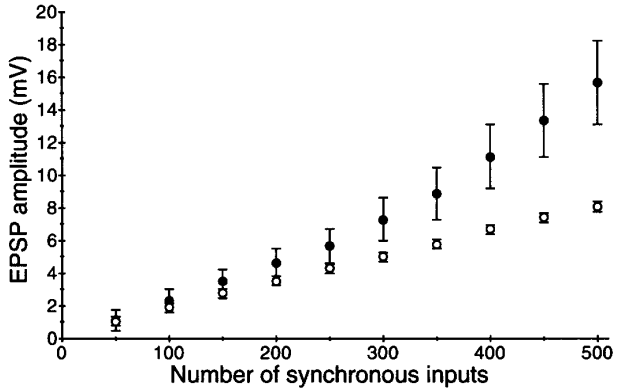

FIG. 3. Effect of number of synchronously activated excitatory inputs on the amplitude of the somatic EPSP (mean ± SD displayed, $n = 200$) for passive dendrite (○) and active dendrite models (●).

to small inputs was dominated by the baseline membrane potential fluctuations (e.g., 1.11 ± 0.62 mV for 50 inputs). When more inputs were activated, the SD of the active model increased with the mean, resulting in a close to constant coefficient of variation (0.17 for 200 inputs, 0.16 for 500 inputs). This constant coefficient of variation confirmed that the amplification of response amplitude and variability were intrinsically linked with each other in the active dendrite model, suggesting a common sensitivity to dendritic excitability.

Robustness of results for changes in background input

The wide range of membrane potentials shown in Fig. 2 was produced by systematically changing the frequencies of the background excitatory and inhibitory input. The effect of these changes on the size and variability of the somatic EPSP in response to a synchronous activation of 200 excitatory inputs is shown in Fig. 4. Remember that the input frequencies of background input used in the model do not represent the firing rate of individual axons (see MODEL AND METHODS).

It is immediately clear that changes in background input frequency had complex effects. Let's first consider the effect on the mean amplitude of the EPSP. In the passive dendrite model (Fig. 4, ○), increasing the background input frequency had two effects: it reduced the input impedance of the model (Bernander et al. 1991; Rapp et al. 1992) and changed the membrane potential to more depolarized (Fig. 4*A*: increasing excitatory frequency) or hyperpolarized (Fig. 4*B*: increasing inhibitory frequency) levels. The reduced input impedance combined with the reduced driving potential for excitatory inputs explains the progressive reduction of the passive dendrite EPSP amplitude in the case of increasing excitatory background frequency. In the case of increased inhibitory frequency, the two effects opposed each other: the reduced input impedance was more than compensated for by an increase in driving potential, causing a slowly increasing EPSP amplitude.

The same effects operated on the active dendrite model, but here the responses also were influenced by the voltage-dependent amplification mechanism. First, below −60 mV average baseline membrane potential (Fig. 4, ▼), the amplification mechanism was not very effective and the active membrane EPSP amplitude was close to the passive one. Above −60 mV (Fig. ●), the amplitude of the EPSP was amplified to a variable extent, depending on the mean baseline membrane potential. In the case of increasing excitatory background frequency (Fig. 4*A*), the amplification mechanism initially overcame the reduced input impedance and driving potential, causing a progressively increasing EPSP amplitude in the active dendrite model (range 16–34 Hz, corresponding to −60 to −50 mV mean baseline membrane

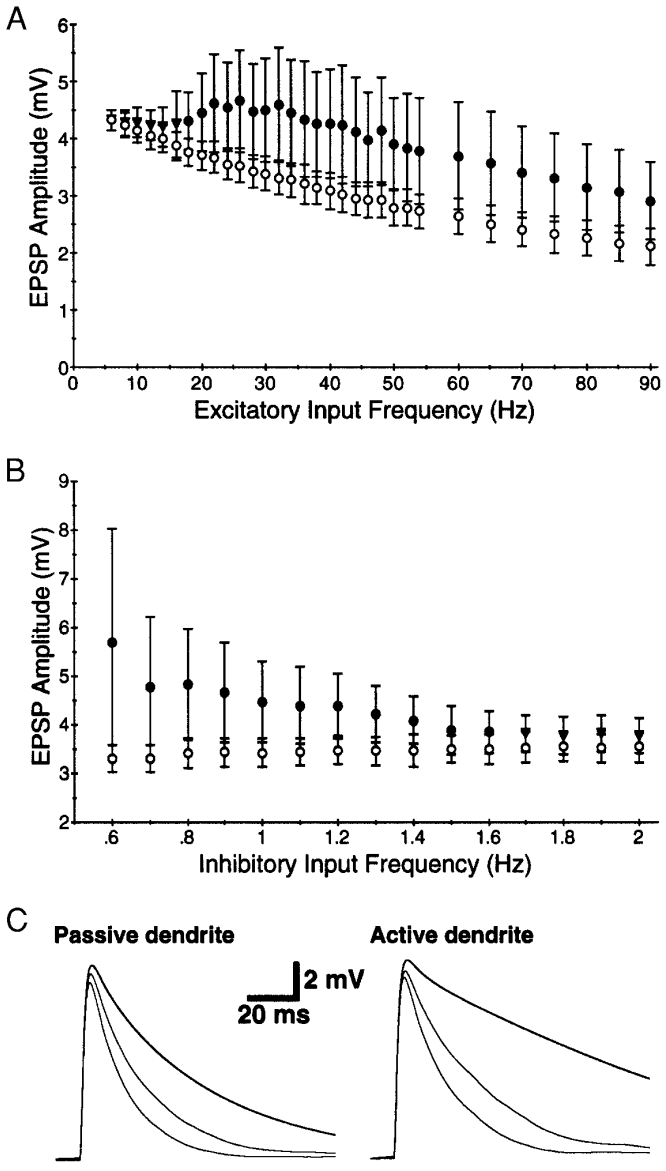

FIG. 4. Effect of changing background input frequency on the amplitude of the somatic EPSP (mean ± SD displayed, n = 200) for passive dendrite (○) and active dendrite models (●, ▼). *A*: excitatory input frequency was increased from 6 to 90 Hz while the inhibitory frequency remained constant at 1 Hz. *B*: inhibitory input frequency was increased from 0.6 to 2.0 Hz while the excitatory frequency remained constant at 28 Hz. *C*: simulation of the effect of blocking background inhibitory input on EPSPs in slice. Two models received either no background synaptic input (top thick lines) or 1- or 2-Hz background inhibition (thin lines). Slice conditions were simulated by the absence of excitatory background input (Häusser and Clark 1997), traces at −78 mV were aligned by somatic injection of current.

potential), whereas that in the passive dendrite model diminished. When the mean baseline membrane potential increased beyond −50 mV, however, the amplification mechanism saturated and the active EPSP amplitude also progressively declined.

A similar effect can be seen in the case of decreasing inhibitory input frequency (Fig. 4*B*): below −60 mV, the EPSPs in the active and passive dendrite models were similar, but beyond −60 mV the somatic EPSPs in the active dendrite model were progressively more amplified. Below 0.6 Hz background inhibition, the active dendrite model started generating dendritic Ca^{2+} spikes in response to the synchronous input, like those seen during current injection in vitro (Llinás and Sugimori 1980a).

In a recent experimental study on the effect of inhibitory background input on Purkinje cell EPSPs (Häusser and Clark 1997), it was concluded that removing background inhibition had a substantial effect on the decay time of the EPSP, roughly doubling it, whereas its amplitude changed only by a few percent. These experimental results confirm the theoretical prediction that background input should affect the time constant much more than it does the input impedance (Rapp et al. 1992; see also Holmes and Woody 1989). In Fig. 4*C*, it is demonstrated that similar results were obtained in both the passive and active dendrite models. Comparison of Fig. 4*C* with Fig. 7*B* of Häusser and Clark (1997) demonstrates that the active dendrite model replicated the experimental data better than the passive one. Specifically, the excitatory input caused a small activation of Ca^{2+} channels in the active dendrite model, which diminished the apparent decay constant compared with that of the passive model. Note, however, that because of the hyperpolarized membrane potential, the activation was insufficient to amplify the EPSP in the active dendrite model.

After explaining the changes in the mean amplitude of the EPSPs, we turn our attention to the changes in SD. For the active dendrite model, Fig. 4 confirmed the results of Fig. 3: whenever the mean amplitude increased, so did the variability of the response (from 0.58 mV at 16 Hz to 0.94 mV at 34 Hz in Fig. 4*A* and from 0.42 mV at 1.6 Hz to 2.35 mV at 0.6 Hz in Fig. 4*B*). When the amplification mechanism saturated (>34 Hz excitatory input frequency in Fig. 4*A*), the SD slowly diminished again (0.67 mV at 90 Hz). For the passive dendrite model, the SD was dominated by the inhibitory component of the background input because of its lower frequency (Jaeger and Bower 1996). As a consequence, the increase in inhibitory driving potential incremented the SD of the EPSPs in the passive membrane model with increasing excitatory input frequency (from 0.19 mV at 6 Hz to 0.32 mV at 90 Hz in Fig. 4*A*). But in Fig. 4*B*, the increase in inhibitory driving potential was more than compensated for by the decrease in inhibitory input frequency, resulting in a slowly decreasing SD (from 0.32 mV at 2 Hz to 0.28 mV at 0.6 Hz). It is also noteworthy that at 52 Hz excitatory background input, the somatic baseline potential of the passive dendrite model approximated that of the active model under standard conditions (−51.2 mV, compare with Fig. 1*B*), but the amplitude of the passive EPSP and its variability (2.80 ± 0.33 mV, Fig. 4*A*) remained much smaller, confirming the fundamental differences between the active and passive models.

Figure 4 clearly demonstrates that the combined amplification of the size and variability of somatic EPSPs in the active dendrite model operated over many background input conditions, provided the mean somatic membrane potential was within the range −60 to −50 mV. This corresponded to the physiological range in vivo (Jaeger and Bower 1994; Jaeger et al. 1997). Although we have shown the robustness over only a limited range of background frequencies, the same was true for much higher or lower input background frequencies (results not shown), provided the membrane potential was in the physiological range (see also De Schutter and Bower 1994b; Jaeger et al. 1997).

Robustness of results for changes in model parameters

After demonstrating the robustness of the variable amplification for changes in the background input, its sensitivity to model parameters will be described. In the original paper describing the model used (De Schutter and Bower 1994a), we described the robustness of the firing evoked by intracellular current injection to changes in the main free parameters of the model, i.e., the maximum conductances ($\bar{g}$) of the voltage and Ca^{2+}-activated channels. The sensitivity of the model synaptic responses to these parameters has never been described, mainly because these responses were considered to be emergent properties of a model that was not specifically tuned to reproduce them (De Schutter 1994). In the present context it is, however, important to demonstrate that the variable amplification mechanism does not depend critically on the fine tuning of the Purkinje cell model.

Figure 5 shows the effect of changing the $\bar{g}$ for a single channel type in all dendritic compartments of the active model for the Ca^{2+} channels (Fig. 5*A*) and for the K^+ channels (Fig. 5*B*). Besides demonstrating the robustness of the model, this figure also indicates which channel types are important in causing the variable amplification. As shown in De Schutter and Bower (1994c), the P-type Ca^{2+} channel was responsible for the amplification of the somatic EPSP. Reducing its $\bar{g}$ led to a progressive reduction of the amplification (Fig. 5*A*, ●) until at 40% of the normal $\bar{g}$, the response could no longer be distinguished from that in a completely passive dendrite. As in Figs. 3 and 4, the variability of the response followed its amplitude, although the coefficient of variation (c.v.) did not remain constant as it did in Fig. 3. This is not surprising as the model c.v. dropped from that of the standard active model (0.19) to that of the standard passive model (0.09) when the $\bar{g}$ of the CaP channels was set to zero. Only modest increases of the $\bar{g}$ for the CaP channels were possible before the model responses became unphysiological. Similar to the effects described in De Schutter and Bower (1994a) increasing the CaP conductance by >30% changed the threshold for dendritic Ca^{2+} spike generation, causing the synchronous input to sometimes evoke full-blown dendritic spikes (▲). This caused a large increase of the SD because the mean response included both normal EPSPs and dendritic spikes of ≥30 mV.

As was demonstrated in De Schutter and Bower (1994c), the T-type Ca^{2+} channel in the model is not involved in the amplification mechanism and changing its $\bar{g}$ had little effect on the amplitude or variability of the somatic EPSP (Fig. 5*A*, ○). The small decrease of EPSP amplitude caused by

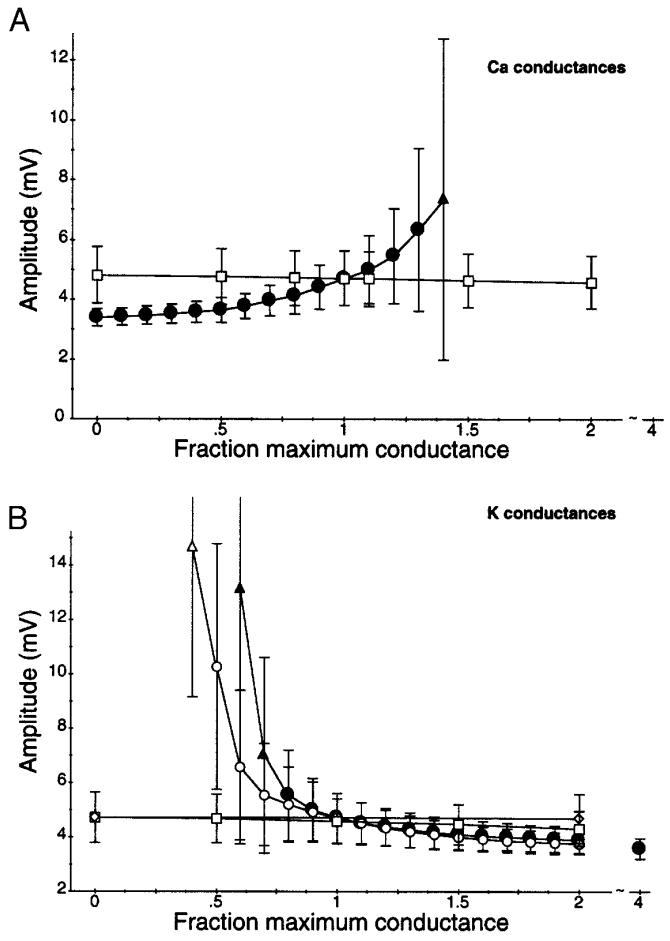

FIG. 5. Effect of changing the densities ($\bar{g}$) of voltage-gated channels on the amplitude of the somatic EPSP (mean ± SD displayed, $n = 200$) for the active dendrite model. *A*: $\bar{g}$ for the P-type (CaP; ● and ▲) and T-type (CaT; □) Ca^{2+} channels were changed relative to their normal value. Increases of the $\bar{g}_{CaP}$ by >30% led to dendritic spiking (▲). *B*: same for the K^+ channels in the model: the Ca^{2+}-activated K^+ channels, BK type (KCa; ● and ▲) and K2 type (K2; ○ and △), and the voltage-gated persistent K^+ channel (◇) and A current (KA; □). Large decreases of the $\bar{g}_{KCa}$ or $\bar{g}_{K2}$ led to dendritic spiking (▲ and △). Note that for the latter, some of the SD bars are not displayed completely. For the simulations, the KA channel was present in the complete dendrite with a constant density indicated relative to the normal in the proximal dendrite (see text).

increasing its $\bar{g}$ can be explained by the progressive depolarization and the effect this had on the amplification mechanism (see Figs. 4 and 8).

In Fig. 5*B*, the effect of changing the $\bar{g}$ of K^+ channels in the model is demonstrated. First, changing the density of voltage-gated K^+ channels had very little effect on the variable amplification. This is demonstrated for the persistent K^+ channel (◇) and for the A-type K^+ channel (□). In the standard model, the A-type channel is present in the proximal smooth dendrite only (De Schutter and Bower 1994a), but because this channel has recently been shown to be important in regulating dendritic excitability in pyramidal cells (Hoffman et al. 1997) and a similar role has been suggested in Purkinje cells (Hounsgaard and Midtgaard 1988; Midtgaard et al. 1993), the simulations shown in Fig. 5*B* used a model with the KA channel present in every dendritic compartment (using the same $\bar{g}$ as in the proximal dendrite for the standard case).

Decreasing the amount of persistent or A-type K^+ conductance in the model had no effect on the variable activation, neither did increasing the amount of persistent K^+ conductance. Increasing the $\bar{g}$ for the KA channels, however, led to a decreased amplification and variability, similar to the effects of decreasing CaP $\bar{g}$ (Fig. 5*A*). A similar and stronger effect was observed for the two Ca^{2+}-activated K^+ conductances in the model, the KCa (Fig. 5*B*, ●) and K2 channels (○). The effect of these three channel types on the amplification mechanism can be explained by their role in dynamically setting the threshold for activation of the CaP channel, as described for the Ca^{2+}-activated K^+ conductances in De Schutter and Bower (1994a). In effect, decreasing the conductance for the Ca^{2+}-activated K^+ conductances had the opposite effect: it increased the amplification and its variability because it enhanced activation of the CaP channel. Eventually the lower threshold for CaP channel activation led again to the generation of full-blown dendritic Ca^{2+} spikes and this at relatively small decreases of $\bar{g}$ for the KCa channel (▲) compared with the decreases necessary for the K2 channel (△). It is unlikely that this difference could be explained by the smaller $\bar{g}$ of the K2 channel in the standard model, as the K2 channel actually generates the largest current when the dendrite is not actively spiking (De Schutter and Bower 1994a). A more probable cause was the intrinsic compensatory dynamics of the K2 channel described in De Schutter and Bower (1994a). Because the K2 channel is activated by small increases in the Ca^{2+} concentration, a decrease of its $\bar{g}$, which leads to more subthreshold CaP activation and more Ca^{2+} influx, will immediately cause a higher activation of the remaining K2 conductance, resulting in a comparatively small decrease in the K2 current.

The results of Fig. 5 demonstrate that whenever the EPSP was amplified, its amplitude was also quite variable and this over a wide range of parameters. But these results did not control for changes in another variable, i.e., the baseline membrane potential. Changing the $\bar{g}$ of the model also modified the average membrane potentials of the model, which by itself will affect the amplification mechanism (Figs. 2 and 8). Therefore an additional series of simulations was run to measure the effect of changing the $\bar{g}$ of the three channel types that caused the most pronounced effects in Fig. 5 (CaP, KCa, and K2) under the condition of a constant baseline membrane potential. The membrane potential was controlled by changing the frequency of the background excitatory input. The findings are shown in Fig. 6, where the white bars reprise the results of Fig. 5, i.e., with changing membrane potential but constant background input, whereas the gray bars show the effect of simultaneously changing the background input to keep the baseline potential constant. For all three conductances, the differences between the two conditions were minimal.

Taken together, Figs. 5 and 6 demonstrate the robustness of the variable amplification to changes in the model parameters as long as sufficient CaP conductance was present to support the amplification mechanism and activation of the CaP channels was not completely suppressed by the Ca^{2+}-activated K^+ channels.

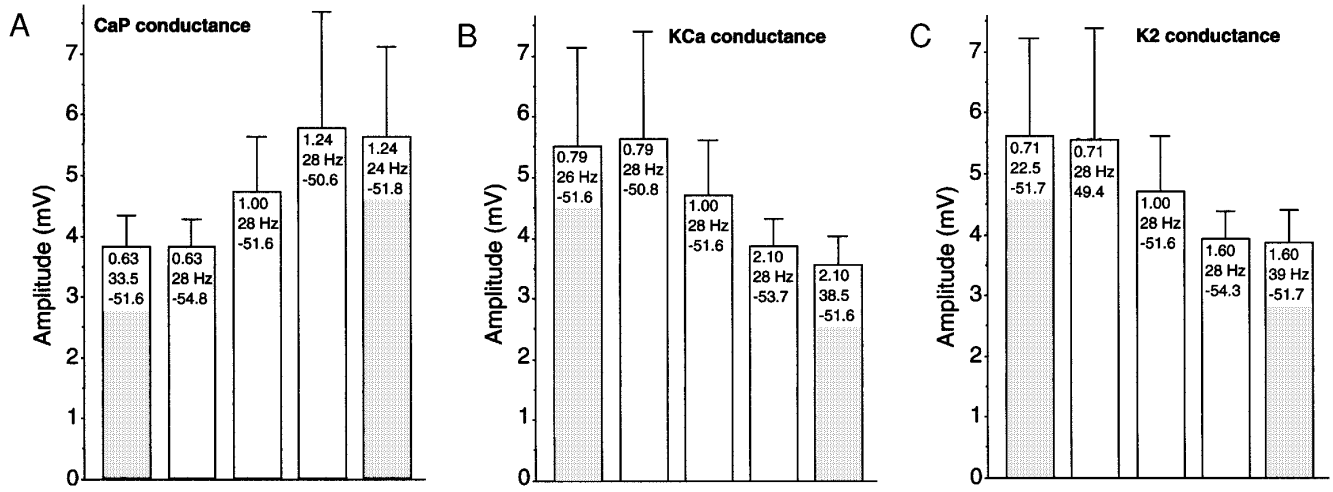

FIG. 6. Effect of somatic membrane voltage on the amplitude of the somatic EPSP in models with changed densities for the voltage-gated channels. *A*: interaction between changes in CaP conductance and membrane voltage. □, replicated data from Fig. 5; they represent, from *left* to *right*, the amplitude of the somatic EPSP (mean ± SD displayed, $n = 200$) for a $\bar{g}$ that reduces the SD to ~50% of its normal value, the standard case, and a $\bar{g}$ that doubles the SD. In each column the relative $\bar{g}$, the frequency of the background excitatory input, and the resulting average somatic membrane potential (in mV) are printed. Note that besides its effect on the amplification, changes of $\bar{g}$ also influenced the baseline membrane potential. ▨, effect shown of changing the frequency of the background excitatory input so as to bring the baseline membrane potential to the same level as in the standard case ($\bar{g} = 1$). *B*: same for changes in the KCa conductance. *C*: same for changes in the K2 conductance.

Time dependence of the variability

The somatic EPSP in response to a synchronous input was highly variable in the active model because its dendritic excitability was not constant (Figs. 1, 3, and 4). This raises the question of how fast this excitability changed. Figure 7*A* shows how the somatic EPSP changed when the synchronous input was provided at different times during an identical pattern of background input. In the active dendrite model, the first three EPSPs in this example had a similar amplitude, even though they started from very different baseline membrane potentials. The fourth and subsequent EPSPs clearly were reduced in amplitude. This example suggests that the dendritic excitability of the active model did not change fast. As expected, the differences in the passive dendrite were much smaller.

To quantify how fast dendritic excitability changed, the baseline membrane potential was autocorrelated over time (Fig. 7*B*, full lines). The autocorrelation of the baseline membrane potential was very different for the passive compared with the active model ($P < 0.001$, paired *t*-test). In the passive model, the autocorrelation function decayed exponentially with a time constant of 35.9 ms, close to the membrane time constant (Jack et al. 1975) of the Purkinje cell (46 ms) (Rapp et al. 1994). The faster decay of the autocorrelation function can be explained by the background synaptic input, which increased the membrane conductance of the model and therefore decreased its time constant. The effects of background synaptic input on the time constant of passive models have been analyzed in detail by others (Bernander et al. 1991; Holmes and Woody 1989; Rapp et al. 1992). Active membrane models do not have a true membrane time constant, but, because of their effect on membrane conductance, activation of ion channels should decrease the ''effective'' (continuously changing) membrane time constant (De Schutter and Bower 1994a; Jack et al. 1975), resulting in a faster decay of the autocorrelation function. Instead, during the first 12 ms, the autocorrelation function of the active dendrite model decreased more slowly than that of the passive model. This then was followed by a much faster decay resulting in a zero correlation after 40 ms. The initially high autocorrelation function of the active dendrite model indicates that changes of dendritic excitability were relatively slow.

The somatic response to synchronous input also was autocorrelated by using simulations similar to that of Fig. 7*A* with the first EPSP as the reference. To facilitate comparison with the baseline membrane potential autocorrelation function, the EPSP peak potential was used. The autocorrelation of the passive dendrite model EPSP peak potentials was identical to that of the baseline membrane potential ($P > 0.85$), reflecting the purely passive membrane time constant effects. For the active dendrite model, the two autocorrelation curves were different ($P < 0.001$), although they clearly overlapped for the critical first 10 ms. The divergence between the two active dendrite autocorrelation curves over longer time intervals can be attributed to activation of dendritic voltage-gated channels by the synchronous synaptic input (De Schutter and Bower 1994c), increasing the nonlinear effects on the autocorrelation curve.

Does the membrane potential predict the amplitude of the response?

Finally we consider the factors causing the increased variability of somatic EPSPs in the active dendrite model. As the amplification process is voltage dependent (Fig. 2) (De Schutter and Bower 1994c), the membrane potential was examined first as a possible predictor of the amplitude of the somatic response to synaptic input. This was not the case

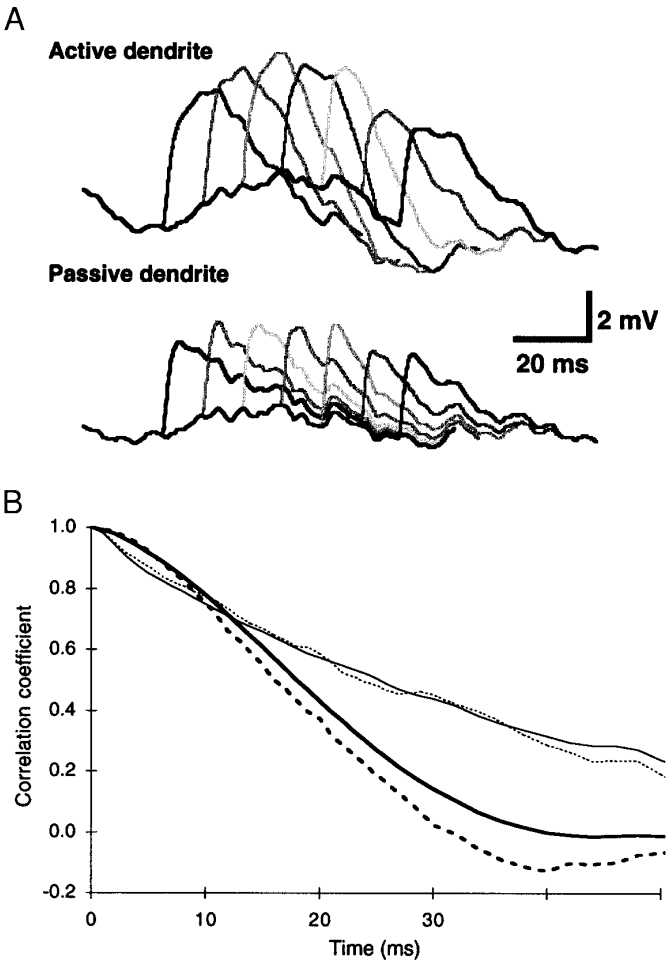

FIG. 7. Changes in dendritic excitability over time. *A*: somatic response produced by providing the synchronous excitatory input at different times (10-ms separation) during identical background input patterns in the active dendrite model (*top*) and passive model (*bottom*). *B*: autocorrelation over time for the baseline membrane potential in the soma (solid lines) and for the EPSP peak potential (dashed lines) for the active (thick lines) and the passive (thin lines) dendrite models.

for the membrane potential at the time of activation of the synchronous input, as it showed no correlation at all with the subsequent EPSP amplitude in the active dendrite model ($r = -0.09$, $n = 2{,}500$; the passive dendrite model showed a weak correlation with $r = -0.31$). This implies that the somatic baseline membrane potential did not reflect the immediate excitability level of the active dendrite.

Because excitability in the model was a dendritic property, the correlation of EPSP amplitude with the dendritic membrane potential averaged over all compartments (e.g., Jaeger et al. 1997) was examined. The mean dendritic membrane potential was, like the somatic membrane potentials, much more variable ($P < 0.001$, 2-sided F test) in the active dendrite (-51.49 ± 1.26 mV, $n = 74$) than in the passive dendrite model (-61.37 ± 0.53 mV). For both the active ($r = -0.16$) and the passive dendrite model ($r = -0.25$), the average dendritic membrane potential at the time of activation of the synchronous input showed a small negative correlation with the amplitude of the somatic EPSP. In the case of the passive dendrite model, this negative correlation reflected the increase in driving potential of synchronous excitatory input at more hyperpolarized levels. In the active dendrite model, it was more relevant to look at the correlation between somatic EPSP amplitude and mean dendritic membrane potential sometime before the synchronous input (Fig. 8). Although the correlation of the passive dendrite model remained relatively constant (up until the time constant, of −36 ms, no statistical difference compared with *time 0* ms: $P > 0.10$, 2-sided F test), it increased in the active dendrite model from −0.16 at *time 0* to −0.61 at time 18 ms before the synchronous input ($P < 0.05$). This increased correlation with dendritic potentials backward in time can be explained by the delays imposed by the (in)activation time constants of the voltage and Ca^{2+}-gated channels. In other words, the background synaptic input had not an immediate effect on the excitability of the dendrite but worked indirectly by first changing the dendritic membrane potential and subsequently the activation of the ionic channels in the dendrite. Note also that both the autocorrelation curve of Fig. 7 and the correlation curve of Fig. 8 turned to zero at ~40 ms after or before the EPSP, respectively, suggesting that this is an important time frame in the variable amplification. Finally, the negative correlation of Fig. 8 shows that the amplification was increased by deactivation and deinactivation of dendritic channels, i.e., relative hyperpolarization increased the size of subsequent EPSPs.

Which dendritic channels are responsible for the variable amplification?

The higher correlation of variable amplification with the past dendritic membrane potential compared with that with the membrane potential at the time of the synchronous input (Fig. 8) suggests that activation of voltage and Ca^{2+}-gated channels was involved, raising the question of which of these channels was most important in determining the excitability. The results of Fig. 5 already pointed to the importance of the CaP channel and of the two Ca^{2+}-activated K^+ channels in the model.

To define the function of these channels more clearly, several strategies were employed. In all cases, the channel (in)activations at the time of the synchronous input were

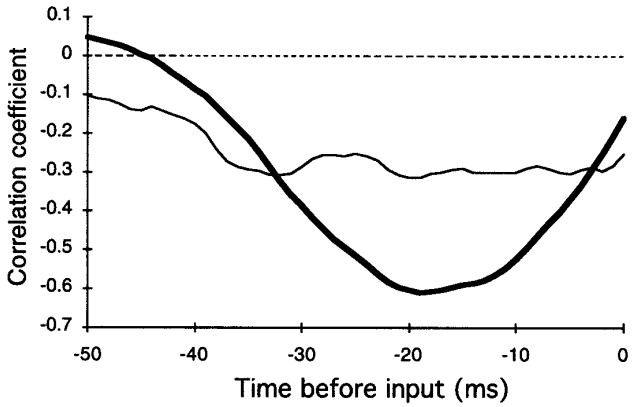

FIG. 8. Correlation of somatic EPSP amplitude with mean dendritic membrane potential at times indicated before the activation of the synchronous input in the active membrane model (thick line) and passive membrane model (thin line).

TABLE 1. *Correlation and variable switching analysis of factors causing variable amplification*

Variable	Correlation with Mean of Factor*	Switching Analysis†	
		Manipulation	Mean Amplitude Difference, mV
		No switch	1.59
		Switch BG	1.23
Excitatory background conductance	0.22	Switch BG + variable	1.19
Inhibitory background conductance	−0.21	Switch BG + variable	1.10
Calcium concentration	−0.19	Switch BG + variable	1.23
V_m-activation CaP channel	−0.19	Switch BG + variable	1.23
V_m-inactivation CaP channel	0.20	Switch BG + variable	1.22
V_m-activation CaT channel	−0.35	Switch BG + variable	1.24
V_m-inactivation CaT channel	0.46	Switch BG + variable	1.21
V_m-activation persistent K channel	−0.49	Switch BG + variable	1.23
V_m-activation KCa channel	−0.17	Switch BG + variable	1.23
V_m-activation K2 channel	−0.14	Switch BG + variable	1.23
Ca-activation KCa channel	−0.47	Switch BG + variable	1.03
Ca-activation K2 channel	−0.46	Switch BG + variable	1.23
Membrane potential (V_m)	−0.16	Switch BG + V_m	1.35
Excitatory background conductance		Switch BG + V_m + variable	1.35
Inhibitory background conductance		Switch BG + V_m + variable	1.57
V_m-activation CaP channel		Switch BG + V_m + variable	1.36
V_m-activation KCa channel		Switch BG + V_m + variable	1.35
V_m-activation K2 channel		Switch BG + V_m + variable	1.35
Ca-activation KCa channel		Switch BG + V_m + variable	0.84
Ca-activation K2 channel		Switch BG + V_m + variable	0.94
		Minimum for any variable	0.33

See text for explanation; BG, background; CaP, P-type Ca^{2+} channel; CaT, T-type Ca^{2+} channel; KCa, BK-type Ca^{2+}-activated channel; K2, K2-type Ca^{2+}-activated channel; V_m, potential. * $n = 74$. † $n = 100$.

studied. This may seem inappropriate as it was just demonstrated that events ≤40 ms *before* the synchronous input determine the size of the amplification (Fig. 8). Here we try to determine, however, if a single model variable can be found that accurately predicts (and controls) at the time of the synchronous input what will be the amplitude of the EPSP. Earlier it was shown that this is not the case for the somatic membrane potential and only poorly so for the average dendritic membrane potential (Fig. 7).

First the activation and inactivation factors of the different dendritic channels were correlated with the amplitude of the resulting somatic EPSP (Table 1, 2nd column). As was shown previously in this model (Jaeger et al. 1997), the background synaptic input has only an indirect effect on the excitability of the dendritic tree, resulting in a low correlation between the activation of excitatory and inhibitory synaptic conductances and the somatic EPSP. For the voltage-gated channels, the correlation analysis of Table 1 would suggest that the most important variables were the voltage-dependent deactivation and deinactivation of the T-type Ca^{2+} channel, deactivation of the persistent K^+ channel, and the Ca^{2+}-deactivation of the Ca^{2+}-activated K^+ channels, because all of these correlations were significantly higher than the negative correlation with the mean dendritic membrane potential. This correlation analysis should be interpreted with caution, however, as the correlations may have been caused indirectly by the correlation with membrane potential (Fig. 8). In fact, it is noticeable that some of the highest correlations were with currents of very small amplitude in the model, i.e., the T-type Ca^{2+} channel and persistent K^+ channel, which were previously shown not to be important for the variable amplification mechanism (Fig. 5). All of the (in)activation factors mentioned had, in the voltage range −60 to −50 mV, an activation time constant of ~10 ms (De Schutter and Bower 1994a). In other words, the most likely explanation for these high correlations is that a high negative correlation with membrane potential ~20 ms before the stimulus (Fig. 8) corresponded to a deactivation or deinactivation of these currents at the time of the synchronous input. It is unlikely that any of these four currents were a causal factor for the variability of amplification.

Because the correlation analysis did not provide conclusive information, a different and new method was employed that we call ''variable switch analysis.'' The variable switch analysis is a sensitive method to identify the causal factors of an effect in a model. First two simulations are selected which produce very different results. Here we are interested in the amplitude of the EPSP, and Fig. 9 shows an example: a *simulation A,* which produced a large EPSP (full black line), and a *simulation B,* which produced a small EPSP to an identical synchronous input. If one assumes that the activation level of a particular channel *X* was completely responsible for the difference in EPSP amplitude between *simulation A* and *B,* then it should be sufficient to replace the activation levels for channel *X* in all compartments of *simulation A* (the ''destination'') with the values of its activation in *simulation B* (the ''source'') to get *simulation A* to produce a small EPSP like in *B.* Vice versa, a switch of the activation levels of *X* from *A* to *B* should cause *simulation B* to produce a large EPSP like in *A.* Because we are trying to find a predictive factor, this switch is effected once only, i.e., at the time of the synchronous input. Subsequent to the switch the changes in activation of channel *X* will be determined by the simulation itself, but because the channel

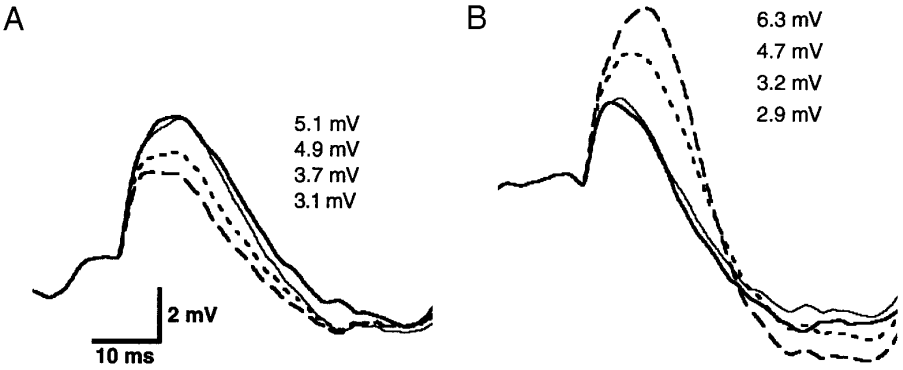

FIG. 9. Example of variable switch analysis. *A* and *B*: somatic EPSP in response to identical synchronous inputs with different background input patterns (thick lines; amplitude 5.1 and 2.9 mV, respectively). Thin traces show the effect of switching the respective patterns of background input between the 2 simulations at the time of activation of the synchronous input. · · ·, effect of switching, in addition to the background, the Ca^{2+}-activation of the Ca^{2+}-activated KCa conductances; – – –, effect of switching both Ca^{2+}-activated K^+ conductances (KCa and K2). Amplitudes of the respective EPSPs are indicated.

time constants are relatively slow compared with the EPSP, such changes in activation will be small and have little effect on the result. Depending on the question asked, the activation of a single channel can be switched, leaving all other model variables untouched, or the activation of several channels can be switched simultaneously.

The practical procedure for the variable switch analysis required selecting a set of pairs of simulations ($n = 50$) with different random number seeds for the background input; this resulted in quite large differences in the EPSP amplitude between the two members of each pair (mean difference 1.59 mV, see example in Fig. 9). The effect of the variable switch analysis was measured as the mean amplitude difference (Table 1, 4th column). The difference was computed between the EPSP amplitudes of the source and the switched destination simulations for all pairs and averaged ($n = 100$ as each member of a pair could be the source). Table 1 shows only the results of the most revealing variable switches, many more were performed (for all channel types in the model).

Before performing the variable switch analysis itself, however, it was necessary to control for the effect of another difference between the two simulations in a pair: the random background input. If the variable amplification was based on a coincidence effect between the background input and the synchronous excitation, a hypothesis that already was refuted by the analysis of Fig. 3, recording the background input in *simulation A* and replaying it in *simulation B* (starting at the time of the synchronous input) should result in *simulation A* producing a small EPSP and vice versa. In the particular example of Fig. 9, replaying the background input had only a small effect on either EPSP. On average, switching the background input reduced the mean difference in EPSP amplitude by only 23% (Table 1, 4th column). This indicates that the variability of the EPSP in the active model was not a coincidence effect, resulting from the summation of background and synchronous synaptic input, as was the case in the passive dendrite model (see analysis of Fig. 3). Nevertheless, because switching the background had some effect, this procedure was included in all the variable switching analyses (Table 1) so as to measure the effect of single variable switches correctly.

The major conclusion from the switch analysis presented in Table 1 was that no single variable consistently controlled the size of the EPSP. In fact, the smallest mean amplitude difference for any single channel switch was 0.84 mV (for V_m + Ca^{2+}-activation of the K2 channel), a decrease of 32% (relative to background only), while the minimum difference possible was 0.33 mV (79% decrease). The latter was computed by finding for each pair which switch produced the smallest difference and then averaging this minimum (which could be from any of the channel activation switches performed) over all pairs. This large difference indicates that no single channel activation was responsible for the size of the EPSP in all simulations. For some pairs, switching a particular variable (e.g., voltage activation of the P-type Ca^{2+} channel) was quite effective in reducing the difference, whereas in most other pairs, it was not.

A close analysis of the results presented in Table 1, top section, shows that the most effective variables in reducing the mean difference were the inhibitory background conductance (mean difference of 11%) and the Ca^{2+}-activation of the KCa channel (16%). It is also quite remarkable that switching the (in)activation of any of the Ca^{2+} channels had little effect at all, in fact the mean difference was identical to that caused by switching the background alone. The effect of switching the background together with the Ca^{2+}-activation of the KCa channel is demonstrated Fig. 9 (· · ·), where this procedure reduced the difference between $EPSP_A$ and $EPSP_B$ by 41% compared with the effect of the background alone. When additionally the Ca^{2+}-activation of the K2 channels was switched (– – –), $EPSP_A$ became almost identical to the original $EPSP_B$ (note the shift in time to peak), while in the case of $EPSP_B$ an overshoot was produced.

For most simulations, the difference increased when, together with the background and the variable itself, the membrane potential in all compartments (V_m) was switched too (Table 1, bottom section). The effect of switching the membrane potential too is that the not only the (in)activation factor but also the driving potential of the channel is switched. The effect of this combined switch was most spectacular for the Ca^{2+}-activation of the two K^+ channels (KCa and K2). Table 1, bottom lines, shows that under these conditions the mean difference was reduced by >30%. In fact an extensive switch of all the activation factors of the Ca^{2+}-activated K^+ channels plus membrane potential and background input resulted in a 50% mean reduction of the difference.

The conclusion is that the causes of the variable excitability are multifactorial but that the most important controlling variables seemed to be the Ca^{2+}-activation of two Ca^{2+}-activated K^+ channels. So although the CaP channel is responsible for the amplification of excitatory inputs, the

Ca^{2+}-activated K^+ channels are important in making this amplification variable.

DISCUSSION

One of the central goals of neurobiology is to understand how neurons process synaptic input and transform it into action potential firing (Shepherd 1990). The simplest description of this process is the integrate-and-fire model, but it is unlikely that such models capture the complexity of real neurons. For example, previous studies have demonstrated that the Purkinje cell model is not an integrate-and-fire model. In fact, the Purkinje cell dendrite is most of the time slightly hyperpolarized compared with the soma, so that the dendrite operates as a current sink (Jaeger et al. 1997). One exception is during the response to a synchronous excitatory input, which activates dendritic voltage-gated Ca^{2+} channels and actively charges the soma (De Schutter and Bower 1994c).

The present study demonstrates that the amplification of EPSPs mediated by these dendritic Ca^{2+} channels is modulated by background input. The primary cause of this modulation was the change in dendritic membrane potential caused by the background input but not at the time at which the excitability was measured (Fig. 8). Instead, there was a strong correlation with the membrane potential tens of milliseconds before. The effect of background input was indirect, operating through changes in activation of voltage and Ca^{2+}-gated channels, which explains why dendritic excitability changed slowly (Fig. 7). That these changes could have such a pronounced effect was not surprising, considering that voltage-gated dendritic currents in the model are much larger than synaptic currents (Jaeger et al. 1997). An extensive analysis (Fig. 9, Table 1) demonstrated that the variability of dendritic excitability could not be attributed to a single channel type. Nevertheless, on average the Ca^{2+}-gated K^+ channels were more important than other ionic channels in the model. The effect of Ca^{2+}-activated K^+ channels also showed the importance of the dendritic Ca^{2+} concentration as a controlling factor of the excitability. This could not be studied in more detail in the present model because Ca^{2+} concentration was computed as a simple exponentially decaying pool (De Schutter and Bower 1994a). More realistic simulations including Ca^{2+} diffusion and buffering (De Schutter and Smolen 1998) will be required to fully investigate the relation between Ca^{2+} concentration and dendritic excitability.

Before discussing the functional implications of these results, the validity of the findings will be considered.

Limitations of the present modeling study

ACCURACY IN MODEL PROPERTIES. A question that always arises with modeling is if the results have relevance to the real system. Of course the final answer to this is experimental verification (see further), but other arguments are relevant too. The main modeling result, i.e., the variable amplification of EPSPs, depended on only two conditions: the presence of amplification by dendritic Ca^{2+} channels and the presence of other voltage- and Ca^{2+}-gated channels that could modulate their activation. It is beyond doubt that dendritic Ca^{2+} and K^+ channels are present in Purkinje cells (Gruol et al. 1991; Llinás and Sugimori 1980a; Usowicz et al. 1992), but do they have the densities and kinetic properties required?

The kinetics of the CaP channel in the model are well constrained by experimental data (Regan 1991; Usowicz et al. 1992; see De Schutter and Bower 1994a), suggesting that these kinetics can indeed support the amplification of EPSPs (see also Fig. 2 of De Schutter and Bower 1994c). The kinetics of the Ca^{2+}-activated K^+ channels in the model are only approximative (De Schutter and Bower 1994a) and therefore may differ from those in real Purkinje cells. But as several K^+ channels support the variable amplification (e.g., Fig. 5 and Table 1), it is likely that changes in their kinetics would change the modeling results only quantitatively (for example the time constants in Figs. 7 and 8), without affecting the main result.

Little is known about the actual densities of dendritic channels in Purkinje cells, but Ca^{2+} imaging shows that at least the Ca^{2+} channels are distributed relatively uniform over the dendrite (Lev-Ram et al. 1992), as in the model. The results from Figs. 5 and 6 suggest that the variable amplification was robust for changes in channel densities but that a minimum density of P-type Ca^{2+} channels was required, and sufficient K^+ channels had to be present to prevent spontaneous dendritic Ca^{2+} spikes. The maximum Ca^{2+} current density in the model is actually lower than that reported experimentally in immature Purkinje cells (Llano et al. 1994), but this may be related to the high specific capacitance used for the model (see Jaeger et al. 1997). Nevertheless, the experimental data (Llano et al. 1994) support the high density of Ca^{2+} channels required for the amplification mechanism and, as predicted by the model (De Schutter and Bower 1994c), focal parallel fiber input can activate those channels (Denk et al. 1995; Eilers et al. 1995). The arguments for high densities of Ca^{2+}-activated K^+ channels is more indirect. It is known that Purkinje cells can be depolarized to fire somatic spikes without generating dendritic Ca^{2+} spikes (Häusser and Clark 1997; Llinás and Sugimori 1980b). It seems logical to expect that the Ca^{2+}-activated K^+ channels that are present in the dendrite (Gruol et al. 1991) and that can be activated by Ca^{2+} at membrane potentials lower than those used in this study (Wang and Augustine 1995) play an important role in suppressing dendritic spikes, though others have suggested that A-type K^+ channels may be important too (Midtgaard et al. 1993).

LIMITATIONS OF THE MODELING APPROACH. Because a passive membrane soma was used in all simulations, synaptically evoked changes in somatic membrane potential and EPSP amplitude could be studied without interference of somatic voltage-gated processes. Although this facilitated the analysis of the modeling results (De Schutter and Bower 1994c), it does not allow for exact predictions of how the variable dendritic excitability changes simple spike firing. Several other voltage-dependent processes may influence action potential firing (Koch et al. 1995), e.g., the refractory period (Jack et al. 1975) and the large Na^+ plateau potentials present in the soma of Purkinje cells (Callaway and Ross 1997; Llinás and Sugimori 1980b). Unfortunately in the model the Na^+ plateau potentials are generated by the window current of the fast Na^+ channel (De Schutter and Bower

1994a), making it impossible to study their effect in absence of spiking.

Another limitation of this study is the simulation of the synaptic input: only 1% of the parallel fiber inputs were simulated (see MODEL AND METHODS), random activation of inputs, etc. (De Schutter and Bower 1994b). Moreover, only one source of noise was considered in the model, i.e., the variability in timing of subthreshold excitatory and inhibitory input, also called the postsynaptic variability (Gossard et al. 1994). Other sources of noise in the preparation, like the stochastic opening of single channels (Hille 1991), stochastic transmitter release (Allen and Stevens 1994), and thermal noise, were not modeled. Because of computational constraints, it was not possible to include the stochastic mechanisms in the computer model, because this would require simulation of each single channel and of each synaptic contact. In experimental recordings, it has been demonstrated that noise can enhance the response to weak inputs (Collins et al. 1996; Pei et al. 1996) and stochasticity of single channel kinetics may be important in this context (Bezrukov and Vodyanoy 1995). Similarly, changes in stochastic transmitter release processes may play an important role in plasticity (Stevens and Wang 1994) and learning. Nevertheless, Fig. 10 demonstrates that the postsynaptic variability caused by subthreshold inputs also may be quite relevant to information processing by the nervous system.

Experimental evidence for variable amplification of EPSPs

Unfortunately the synaptic amplification mechanism in Purkinje cells has not yet been studied experimentally, although evidence for synaptic activation of dendritic Ca^{2+} channels exists (Denk et al. 1995; Eilers et al. 1995). These studies are limited, however, by the absence of excitatory background input in the cerebellar slice preparation (Häusser and Clark 1997) and by the relative hyperpolarized membrane potentials at which the cells are studied. A recent experimental study demonstrated, however, the importance of background inhibition in controlling interspike interval distributions (Häusser and Clark 1997), as was predicted by the model (De Schutter and Bower 1994b; Jaeger et al. 1997). Moreover, it was shown in this paper (Fig. 4*C*) that background inhibition had the same effect on the integration of excitatory synaptic input by the active dendrite model as in the experimental study (Fig. 7*B* of Häusser and Clark 1997).

In many other neurons, like pyramidal cells in the neocortical slice preparation, changes in EPSP shapes due to voltage-gated activation of dendritic conductances have been reported (Deisz et al. 1991; Markram and Sakmann 1994; Nicoll et al. 1993; Schwindt and Crill 1997; Seamans et al. 1997), and the resulting amplification is quite variable (Deisz et al. 1991). Other systems where amplification of excitatory synaptic inputs have been reported are hippocampal pyramidal cells (Gillessen and Alzheimer 1997; Lipowsky et al. 1996) and fly visual neurons (Haag and Borst 1996). More relevant to the present modeling study are in vivo intracellular recordings of neurons. Membrane potential fluctuations are very large in in vivo recordings of pyramidal neurons from cat visual cortex (Ferster and Jagadeesh 1992) and monkey sensorimotor cortex (Murthy and Fetz 1992).

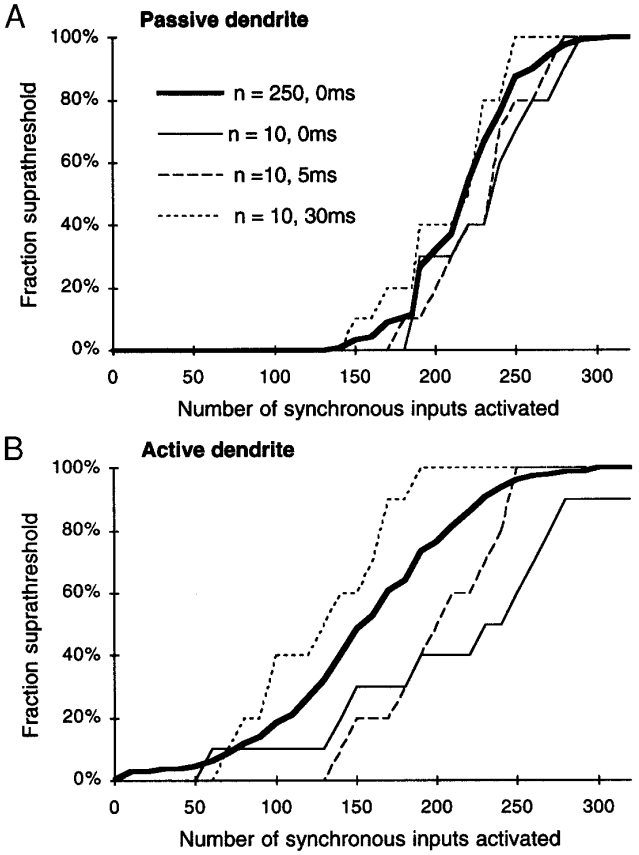

FIG. 10. Functional importance of amplification of postsynaptic variability by active dendrites. *A*: fraction of suprathreshold EPSPs evoked by different-sized synchronous inputs in the passive dendrite model. Fraction computed for a large sample of different background input patterns (n = 250, thick line) is shown together with the fractions for a smaller sample (n = 10) where the synchronous input was activated at different times (0 ms, 5 or 30 ms). *B*: fraction of suprathreshold EPSPs in the active dendrite model; same conventions as in *A*.

Moreover, these fluctuations ''can distort the EPSP's shape'' significantly (Ferster and Jagadeesh 1992), and the amplitude of EPSPs is quite variable (coefficient of variation of 58% reported by Matsumura et al. 1996).

It has been known for quite some time that spinal cord α-motoneurons show in vivo a ''postsynaptic'' variability of EPSP amplitudes that is caused by background synaptic input (Gossard et al. 1994). In these neurons, the activation of a dendritic plateau potential in vivo evokes a large increase of the somatic membrane potential noise (Hounsgaard et al. 1988). Although the origin of this increased membrane potential noise has not been determined, our simulation results suggest that it may be caused by increased membrane potential fluctuations due to the activation of the dendritic Ca^{2+} channels that cause the plateau potential and that move the neuron to an active dendrite state (e.g., Fig. 1*B*).

Finally, it should be mentioned that recent improvements in experimental recording techniques have led to substantial evidence of synaptically evoked subthreshold activation of dendritic voltage-gated channels in pyramidal cells (Magee and Johnston 1995); this can lead to localized Ca^{2+} inflow in the dendrite (Markram and Sakmann 1994; Regehr and Tank 1992). Moreover, it was recently shown that a den-

dritic A-type K^+ channel can control dendritic excitability in these cells (Hoffman et al. 1997). In the Purkinje cell model, Ca^{2+}-activated K^+ channels were more important in this regard than A channels (Fig. 5*B*).

Functional consequences of variable amplification of EPSPs

CONSEQUENCES IN GENERAL. What are the functional consequences of the amplification of postsynaptic variability? A simple analysis of the effect on spike initiation is presented in Fig. 10, where the thick lines show the fraction of suprathreshold responses caused by different sized synchronous stimuli in the passive dendrite model versus the active one. The slopes of these curves reflect the background induced variability in the system, as with a steady membrane potential and constant amplification, the fraction of suprathreshold responses would jump from 0 to 100%. The much more shallow response curve in Fig. 10*B* demonstrates that the active dendrite model behaved quite differently from the passive one. The 10–90% fraction suprathreshold responses spanned a difference of 160 synchronous inputs in the active dendrite model, compared with only 80 in the passive model. It should be noted that the data in Fig. 10 also can be interpreted as the mean response of a population of neurons receiving an identical synchronous input but different background input.

The shallow slope of the response curve means that it is more difficult to predict for neurons with an active dendrite if a particular coherent input will be effective in firing the cell or not, whereas there is little variability in the response of a passive dendrite. Although this could suggest that neurons with an active dendrite are less reliable, it implies that these neurons perform more complex computations on their input, resulting in an increased information processing capacity. In fact, the background synaptic input had a much larger effect on the subsequent responses of an active dendrite neuron than was the case with a passive dendrite (Figs. 7 and 8). In other words, passive neurons largely ''threw away'' their subthreshold synaptic inputs, whereas an active dendrite integrated them by changing its excitability. This caused a change in excitability over time that also was reflected in the response curves of the active dendrite. In the analysis of Fig. 10, the shift over time becomes visible when only a small number of simulations was used to compute the response curve (thin lines). It is clear that in the active dendrite model such response curves were different from the large averaged one (thick line of Fig. 10*B*). Conversely, in the passive dendrite all the response curves largely overlapped. Moreover, for the active dendrite model the two curves taken at 0 and 5 ms were much more similar to each other than those taken at 0 and 30 ms. This was to be expected from the results of Fig. 7*B*, which predict that changes in timing of the synchronous input by $\leq$10 ms have very small effects on the response, whereas delays by $\geq$30 ms completely reset the dendritic excitability (zero correlation). In other words, a small delay of a few milliseconds in the timing of a coherent input (e.g., Nelson et al. 1992) will not change the response, but shifts in timing of $>$30 ms can have a profound effect.

To summarize, the variable amplification allows background input to slowly change the effective threshold of the cell (or population) for spiking in response to coherent input.

CONSEQUENCES FOR CEREBELLAR FUNCTION. This leads to specific predictions on cerebellar function when the cerebellar anatomy is considered. A crucial question in understanding synaptic integration by Purkinje cells is the effectiveness of single parallel fiber inputs. Classic theories of cerebellar function (Albus 1971; Braitenberg et al. 1997; Marr 1969) propose that thousands of the 150,000 parallel fiber inputs onto a single Purkinje cell (Harvey and Napper 1991) have to be coactivated to cause a response. Such a large stimulus would be very reliable as it is outside of the range where variable amplification has any effect (Fig. 10). But recent experimental findings suggest that much smaller stimuli also might be adequate. Barbour (1993) estimated that 50 parallel fiber inputs might be sufficient to cause the Purkinje cell to fire a spike. Similarly, activation of a few (Eilers et al. 1995) or even a single (Denk et al. 1995) parallel fiber is enough to activate dendritic Ca^{2+} channels. But if the Purkinje cell is so sensitive to activation of a small number of its 150,000 excitatory synapses, what prevents it from firing continuously at maximum rate? Analysis of the Purkinje cell model has shown that the feed-forward inhibition by stellate cells, which also receive parallel fiber input (Ito 1984; Palay and Chan-Palay 1974), can cancel the constant component of parallel fiber activation (Jaeger et al. 1997). In fact under conditions of steady background input, the Purkinje model settles at an average membrane potential where the inhibitory current is larger than the excitatory one. I previously have proposed that long-term depression of the parallel fiber synapse may be important in fine-tuning this balance between excitation and inhibition (De Schutter 1995a, 1997).

Although the average firing rate of the model will be determined by the balance between excitation and inhibition, its instantaneous firing rate is very sensitive to sudden changes in the rate of parallel fiber input. For example, if a small synchronous input of $\sim$150 parallel fibers is added to the background excitation and inhibition, it often will evoke a spike (De Schutter 1994) (Figs. 3 and 10*B*). Such synchronous inputs are presumably not canceled by inhibition because the feed-forward loop acts with a delay. Assuming that activation by small synchronous excitatory inputs is a correct representation of Purkinje cell function, its response will be very sensitive to the variable thresholds demonstrated in Fig. 10.

An exact functional description requires an identification of the respective sources and activation patterns of the synchronous input versus asynchronous background input in cerebellar cortex. I previously have proposed that background excitation would be provided by parallel fibers and background dendritic inhibition by stellate cells (De Schutter and Bower 1994b,c). Similarly, the synchronous input could be provided by the ascending branch of the granule cell axon (Bower 1997), which makes much more extensive synaptic contacts with close by Purkinje cells than has been generally assumed (Gundappa-Sulur et al. 1998), or by the parallel fibers (Braitenberg et al. 1997). Because of their long length ($\leq$5 mm long) (Mugnaini 1983; Pichitpornchai et al. 1994), parallel fibers originate in many different patches of the fractured somatotopy of cerebellar cortex (Shambes et al. 1978) and consequently will carry information from many different sources, while ascending branches are expected to convey one particular receptive modality only (Bower 1997;

Bower and Woolston 1983). If this functional separation of the granule axon in an ascending and parallel branch is correct, the parallel fiber system transmits heterogenous background input, which, by the variable amplification mechanism, can modulate the Purkinje cell response to synchronous excitation by the homogenous ascending branch input. As is demonstrated in Fig. 10*B*, the parallel fiber system (combined with feed-forward inhibition by stellate cells) can change the effective threshold for spike transmission by ascending branch inputs. In other words, the parallel fiber system may determine if a particular mossy fiber input can activate the overlying Purkinje cells by gating the ascending branch input.

In the context of this theory, the Purkinje cell does not act as a coincidence detector as it is insensitive to the exact timing of the ascending branch input (Figs. 7*B* and 10*B*). This is in contradiction with other theories (Braitenberg and Atwood 1958; Braitenberg et al. 1997), which assume that the Purkinje cell operates as a detector of parallel fiber coincidences. It indeed can be shown that Purkinje cell responses to large synchronous activations of the parallel fiber tract in vitro are time locked (Heck 1994), but as argued above and elsewhere (Jaeger and De Schutter 1997) it is unlikely that these stimulation paradigms are physiological.

Although the gating theory of parallel fiber function presented here (see also Bower 1997) is attractive, many unknowns remain. In particular, the timing of granule cell activation may be much less random than is generally assumed (Maex et al. 1996; Vos et al. 1997). Similarly, the activation patterns of the stellate cells, which are crucial in determining Purkinje cell spiking responses (Jaeger and Bower 1996; Jaeger et al. 1997), have not been determined in vivo.

I thank J. M. Bower for access to the Intel Touchstone Delta System operated by Caltech on behalf of the Concurrent Supercomputing Consortium and anonymous reviewers for valuable comments.

This work was supported by Fonds Wetenschappelijk Onderzoek (Flanders) and National Institute of Mental Health Grant MH-52903.

Received 8 September 1997; accepted in final form 29 April 1998.

REFERENCES

ALBUS, J. S. A theory of cerebellar function. *Math. Biosci.* 10: 25–61, 1971.

ALLEN, C. AND STEVENS, C. F. An evaluation of causes for unreliability of synaptic transmission. *Proc. Natl. Acad. Sci. USA* 91: 10380–10383, 1994.

AMITAI, Y., FRIEDMAN, A., CONNORS, B. W., AND GUTNICK, M. J. Regenerative activity in apical dendrites of pyramidal cells in neocortex. *Cereb. Cortex* 3: 26–38, 1993.

BARBOUR, B. Synaptic currents evoked in Purkinje cells by stimulating individual granule cells. *Neuron* 11: 759–769, 1993.

BERNANDER, Ö., DOUGLAS, R. J., MARTIN, K.A.C., AND KOCH, C. Synaptic background activity influences spatiotemporal integration in single pyramidal cells. *Proc. Natl. Acad. Sci. USA* 88: 11569–11573, 1991.

BEZRUKOV, S. M. AND VODYANOY, I. Noise induced enhancement of signal transduction across voltage-dependent ion channels. *Nature* 378: 362–364, 1995.

BOWER, J. M. Is the cerebellum sensory for motor's sake or motor for sensory's sake: the view from the whiskers of a rat? *Prog. Brain Res.* 114: 463–496, 1997.

BOWER, J. M. AND BEEMAN, D. *The book of GENESIS: exploring realistic neural models with the GEneral NEural SImulation System.* New York: TELOS, 1995.

BOWER, J. M. AND WOOLSTON, D. C. Congruence of spatial organization of tactile projections to granule cell and Purkinje cell layers of cerebellar hemispheres of the albino rat: vertical organization of cerebellar cortex. *J. Neurophysiol.* 49: 745–766, 1983.

BRAITENBERG, V. AND ATWOOD, R. P. Morphological observations on the cerebellar cortex. *J. Comp. Neurol.* 109: 1–33, 1958.

BRAITENBERG, V., HECK, D., AND SULTAN, F. The detection and generation of sequences as a key to cerebellar function. Experiments and theory. *Behav. Brain Sci.* 20: 229–245, 1997.

CALLAWAY, J. C. AND ROSS, W. N. Spatial distribution of synaptically activated sodium concentration changes in cerebellar Purkinje neurons. *J. Neurophysiol.* 77: 145–152, 1997.

COLLINS, J. J., IMHOFF, T. T., AND GRIGG, P. Noise enhanced information transmission in rat SA1 cutaneous mechanoreceptors via aperiodic stochastic resonance. *J. Neurophysiol.* 76: 642–645, 1996.

DE SCHUTTER, E. Modelling the cerebellar Purkinje cell: Experiments in computo. *Prog. Brain Res.* 102: 427–441, 1994.

DE SCHUTTER, E. Cerebellar long-term depression might normalize excitation of Purkinje cells: a hypothesis. *Trends Neurosci.* 18: 291–295, 1995a.

DE SCHUTTER, E. Dendritic calcium channels amplify the variability of postsynaptic responses. *Soc. Neurosci. Abstr.* 21: 586, 1995b.

DE SCHUTTER, E. A new functional role for cerebellar long term depression. *Prog. Brain Res.* 114: 529–542, 1997.

DE SCHUTTER, E. AND BOWER, J. M. Parallel fiber input modulates Purkinje cell responses to ascending fiber granule cell input. *Soc. Neurosci. Abstr.* 18: 407, 1992.

DE SCHUTTER, E. AND BOWER, J. M. Integration of synaptic inputs in a model of the Purkinje cell. In: *Computation and Neural Systems*, edited by F. H. Eeckman and J. M. Bower. Norwell, MA: Kluwer Academic, 1993, p. 355–362.

DE SCHUTTER, E. AND BOWER, J. M. An active membrane model of the cerebellar Purkinje cell. I. Simulation of current clamps in slice. *J. Neurophysiol.* 71: 375–400, 1994a.

DE SCHUTTER, E. AND BOWER, J. M. An active membrane model of the cerebellar Purkinje cell. II. Simulation of synaptic responses. *J. Neurophysiol.* 71: 401–419, 1994b.

DE SCHUTTER, E. AND BOWER, J. M. Simulated responses of cerebellar Purkinje cells are independent of the dendritic location of granule cell synaptic inputs. *Proc. Natl. Acad. Sci. USA* 91: 4736–4740, 1994c.

DE SCHUTTER, E. AND SMOLEN, P. Calcium dynamics in large neuronal models. In: *Methods in Neuronal Modeling: From Synapses to Networks*, edited by C. Koch and I. Segev (2nd ed.). Cambridge, MA: MIT Press, 1998, p. 212–249.

DEISZ, R. A., FORTIN, G., AND ZIEGLGÄNSBERGER, W. Voltage dependence of excitatory postsynaptic potentials of rat neocortical neurons. *J. Neurophysiol.* 65: 371–382, 1991.

DENK, W., SUGIMORI, M., AND LLINÁS, R. R. 2 types of calcium response limited to single spines in cerebellar Purkinje cells. *Proc. Natl. Acad. Sci. USA* 92: 8279–8282, 1995.

DESTEXHE, A., CONTRERAS, D., STERIADE, M., SEJNOWSKI, T. J., AND HUGUENARD, J. R. In vivo, in vitro and computational analysis of dendritic calcium currents in thalamic reticular neurons. *J. Neurosci.* 16: 169–185, 1996.

EILERS, J., AUGUSTINE, G. J., AND KONNERTH, A. Subthreshold synaptic Ca^{2+} signaling in fine dendrites and spines of cerebellar Purkinje neurons. *Nature* 373: 155–158, 1995.

FERSTER, D. AND JAGADEESH, B. EPSP-IPSP interactions in cat visual cortex studied with in vivo whole-cell patch recordings. *J. Neurosci.* 12: 1262–1274, 1992.

GÄHWILER, B. H. AND LLANO, I. Sodium and potassium conductances in somatic membranes of rat Purkinje cells from organotypic cerebellar cultures. *J. Physiol. (Lond.)* 417: 105–122, 1989.

GILLESSEN, T. AND ALZHEIMER, C. Amplification of EPSPs by low Ni^{2+}- and amiloride sensitive Ca^{2+} channels in apical dendrites of rat CA1 pyramidal neurons. *J. Neurophysiol.* 77: 1639–1643, 1997.

GOSSARD, J. P., FLOETER, M. K., KAWAI, Y., BURKE, R. E., CHANG, T., AND SCHIFF, S. J. Fluctuations of excitability in the monosynaptic reflex pathway to lumbar motoneurons in the cat. *J. Neurophysiol.* 72: 1227–1239, 1994.

GRUOL, D. L., JACQUIN, T., AND YOOL, A. J. Single-channel K^+ currents recorded from the somatic and dendritic regions of cerebellar Purkinje neurons in culture. *J. Neurosci.* 11: 1002–1015, 1991.

GUNDAPPA-SULUR, G., DE SCHUTTER, E., AND BOWER, J. M. The ascending branch of the granule cell axon: an important component of the cerebellar cortical circuitry. *J. Comp. Neurol.* In press.

HAAG, J. AND BORST, A. Amplification of high-frequency synaptic input by active dendritic membrane processes. *Nature* 379: 639–641, 1996.

HARVEY, R. J. AND NAPPER, R.M.A. Quantitative studies of the mammalian cerebellum. *Prog. Neurobiol.* 36: 437–463, 1991.

HÄUSSER, M. AND CLARK, B. A. Tonic synaptic inhibition modulates neuronal output pattern and spatiotemporal integration. *Neuron* 19: 665–678, 1997.

HECK, D. Rat cerebellar cortex in vitro responds specifically to moving stimuli. *Neurosci. Lett.* 157: 95–98, 1994.

HILLE, B. *Ionic Channels of Excitable Membranes.* Sunderland, MA: Sinauer, 1991.

HOFFMAN, D. A., MAGEE, J. C., COLBERT, C. M., AND JOHNSTON, D. K^+ channel regulation of signal propagation in dendrites of hippocampal pyramidal neurons. *Nature* 387: 869–875, 1997.

HOLMES, W. R. AND WOODY, C. D. Effects of uniform and non-uniform synaptic ''activation-distributions'' on the cable properties of modeled cortical pyramidal neurons. *Brain Res.* 505: 12–22, 1989.

HOUNSGAARD, J., HULTBORN, H., JESPERSEN, B., AND KIEHN, O. Bistability of α-motoneurones in the decerebrate cat and in the acute spinal cat after intravenous 5-hydroxytryptophan. *J. Physiol. (Lond.)* 405: 345–367, 1988.

HOUNSGAARD, J. AND MIDTGAARD, J. Intrinsic determinants of firing patterns in Purkinje cells of the turtle cerebellum in vitro. *J. Physiol. (Lond.)* 402: 731–749, 1988.

ITO, M. *The Cerebellum and Neural Control.* New York: Raven, 1984.

JACK, J.J.B., NOBLE, D., AND TSIEN, R. W. *Electric Current Flow in Excitable Cells.* Oxford, UK: Clarendon, 1975.

JAEGER, D. AND BOWER, J. M. Prolonged responses in rat cerebellar Purkinje cells following activation of the granule cell layer: an intracellular in vitro and in vivo investigation. *Exp. Brain Res.* 100: 200–214, 1994.

JAEGER, D. AND BOWER, J. M. Function of background synaptic input in cerebellar Purkinje cells explored with dynamic current clamping. *Soc. Neurosci. Abstr.* 22: 494, 1996.

JAEGER, D. AND DE SCHUTTER, E. Anatomical structure alone can not predict function. *Behav. Brain Sci.* 20: 252, 1997.

JAEGER, D., DE SCHUTTER, E., AND BOWER, J. M. The role of synaptic and voltage-gated currents in the control of Purkinje cell spiking: a modeling study. *J. Neurosci.* 17: 91–106, 1997.

KANEDA, M., WAKAMORI, M., ITO, M., AND AKAIKE, N. Low-threshold calcium current in isolated Purkinje cell bodies of rat cerebellum. *J. Neurophysiol.* 63: 1046–1051, 1990.

KOCH, C., BERNANDER, Ö., AND DOUGLAS, R. Do neurons have a voltage or a current threshold for action potential initiation? *J. Comput. Neurosci.* 2: 63–82, 1995.

LATORRE, R., OBERHAUSER, A., LABARCA, P., AND ALVAREZ, O. Varieties of calcium-activated potassium channels. *Annu. Rev. Physiol.* 51: 385–399, 1989.

LEV-RAM, V., MIYAKAWA, H., LASSER-ROSS, N., AND ROSS, W. N. Calcium transients in cerebellar Purkinje neurons evoked by intracellular stimulation. *J. Neurophysiol.* 68: 1167–1177, 1992.

LIPOWSKY, R., GILLESSEN, T., AND ALZHEIMER, C. Dendritic Na^+ channels amplify EPSPs in hippocampal CA1 pyramidal cells. *J. Neurophysiol.* 76: 2181–2191, 1996.

LLANO, I., DIPOLO, R., AND MARTY, A. Calcium-induced calcium release in cerebellar Purkinje cells. *Neuron* 12: 663–673, 1994.

LLINÁS, R. R. AND SUGIMORI, M. Electrophysiological properties of in vitro Purkinje cell dendrites in mammalian cerebellar slices. *J. Physiol. (Lond.)* 305: 197–213, 1980a.

LLINÁS, R. R. AND SUGIMORI, M. Electrophysiological properties of in vitro Purkinje cell somata in mammalian cerebellar slices. *J. Physiol. (Lond.)* 305: 171–195, 1980b.

LLINÁS, R. R., SUGIMORI, M., AND CHERKSEY, B. Voltage-dependent calcium conductances in mammalian neurons: the P channel. *Ann. NY Acad. Sci.* 560: 103–111, 1989.

MAEX, R., VOS, B. P., AND DE SCHUTTER, E. Dynamics of a detailed model of the granular layer of the cerebellum. *Soc. Neurosci. Abstr.* 22: 1093, 1996.

MAGEE, J. C. AND JOHNSTON, D. Synaptic activation of voltage-gated channels in the dendrites of hippocampal pyramidal neurones. *Science* 268: 301–304, 1995.

MARKRAM, H. AND SAKMANN, B. Calcium transients in apical dendrites evoked by single subthreshold excitatory postsynaptic potentials via low-voltage-activated calcium channels. *Proc. Natl. Acad. Sci. USA* 91: 5207–5211, 1994.

MARR, D. A. A theory of cerebellar cortex. *J. Physiol. (Lond.)* 202: 437–470, 1969.

MATSUMURA, M., CHEN, D.-F., SAWAGUCHI, T., KUBOTA, K., AND FETZ, E. E. Synaptic interactions between primate precentral cortex neurons revealed by spike-triggered averaging of intracellular membrane potentials in vivo. *J. Neurosci.* 16: 7757–7767, 1996.

MIDTGAARD, J., LASSER-ROSS, N., AND ROSS, W. N. Spatial distribution of Ca^{2+} influx in turtle Purkinje cell dendrites in vitro: role of a transient outward current. *J. Neurophysiol.* 70: 2455–2469, 1993.

MUGNAINI, E. The length of cerebellar parallel fibers in chicken and rhesus monkey. *J. Comp. Neurol.* 220: 7–15, 1983.

MURTHY, V. N. AND FETZ, E. E. Coherent 25 Hz to 35 Hz oscillations in the sensorimotor cortex of awake behaving monkeys. *Proc. Natl. Acad. Sci. USA* 89: 5670–5674, 1992.

NELSON, J. I., SALIN, P. A., MUNK, M.H.J., ARZI, M., AND BULLIER, J. Spatial and temporal coherence in corticocortical connections. A cross-correlation study in area 17 and area 18 in the cat. *Vis. Neurosci.* 9: 21–37, 1992.

NICOLL, A., LARKMAN, A., AND BLAKEMORE, C. Modulation of EPSP shape and efficacy by intrinsic membrane conductances in rat neocortical pyramidal neurons in vitro. *J. Physiol. (Lond.)* 468: 693–710, 1993.

PALAY, S. L. AND CHAN-PALAY, V. *Cerebellar Cortex*. New York: Springer-Verlag, 1974.

PARÉ, D. AND LEBEL, E. L. Differential impact of miniature synaptic potentials on the soma and dendrites of pyramidal neurons in vivo. *J. Neurophysiol.* 77: 1735–1739, 1997.

PEI, X., WILKENS, L. A., AND MOSS, F. Light enhances hydrodynamic signaling in the multimodal caudal photoreceptor interneurons of the crayfish. *J. Neurophysiol.* 76: 3002–3011, 1996.

PICHITPORNCHAI, C., RAWSON, J. A., AND REES, S. Morphology of parallel fibers in the cerebellar cortex of the rat: an experimental light and electron microscopic study with biocytin. *J. Comp. Neurol.* 342: 206–220, 1994.

RAPP, M., SEGEV, I., AND YAROM, Y. Physiology, morphology and detailed passive models of guinea-pig cerebellar Purkinje cells. *J. Physiol. (Lond.)* 474: 101–118, 1994.

RAPP, M., YAROM, Y., AND SEGEV, I. The impact of parallel fiber background activity on the cable properties of cerebellar Purkinje cells. *Neural Comput.* 4: 518–533, 1992.

REGAN, L. J. Voltage-dependent calcium currents in Purkinje cells from rat cerebellar vermis. *J. Neurosci.* 11: 2259–2269, 1991.

REGEHR, W. G. AND TANK, D. W. Calcium concentration dynamics produced by synaptic activation of CA1 hippocampal pyramidal cells. *J. Neurosci.* 12: 4202–4223, 1992.

SCHWINDT, P. C. AND CRILL, W. E. Local and propagated dendritic action potentials evoked by glutamate iontophoresis on rat neocortical pyramidal neurons. *J. Neurophysiol.* 77: 2466–2486, 1997.

SEAMANS, J. K., GORELOVA, N. A., AND YANG, C. R. Contributions of voltage-gated Ca^{2+} channels in the proximal versus distal dendrites to synaptic integration in prefrontal cortical neurons. *J. Neurosci.* 17: 5936–5948, 1997.

SHAMBES, G. M., GIBSON, J. M., AND WELKER, W. Fractured somatotopy in granule cell tactile areas of rat cerebellar hemispheres revealed by micromapping. *Brain Behav. Evol.* 15: 94–140, 1978.

SHEPHERD, G. M. *The Synaptic Organization of the Brain.* New York: Oxford, 1990.

SOFTKY, W. R. AND KOCH, C. The highly irregular firing of cortical cells is inconsistent with temporal integration of EPSPs. *J. Neurosci.* 13: 334–350, 1993.

STEVENS, C. F. AND WANG, Y. Y. Changes in reliability of synaptic function as a mechanism for plasticity. *Nature* 371: 704–707, 1994.

STUART, G. AND HÄUSSER, M. Initiation and spread of sodium action potentials in cerebellar Purkinje cells. *Neuron* 13: 703–712, 1994.

SULTAN, F., ELLISMAN, M. H., AND BOWER, J. M. Quantitative anatomical aspects of the inhibitory interneurons of the rat cerebellar molecular layer: a light and electron microscopic Golgi study. *Soc. Neurosci. Abstr.* 21: 1191, 1995.

USOWICZ, M. M., SUGIMORI, M., CHERKSEY, B., AND LLINÁS, R. R. P-type calcium channels in the somata and dendrites of adult cerebellar Purkinje cells. *Neuron* 9: 1185–1199, 1992.

VOS, B. P., MAEX, R., AND DE SCHUTTER, E. Correlation of firing between rat cerebellar Golgi cells. *Soc. Neurosci. Abstr.* 23: 1286, 1997.

WANG, S.S.-H. AND AUGUSTINE, G. J. Local regulation of dendritic physiology by photolysis of caged calcium. *Soc. Neurosci. Abstr.* 21: 590, 1995.